

## CFD-Based Airside Heat Transfer and Pressure Drop Correlation Development for Small Diameter (3 mm to 5 mm) Louver Fin Heat Exchangers

Shekhar SARPOTDAR<sup>1\*</sup>, Dennis NASUTA<sup>2</sup>, Vikrant AUTE<sup>3</sup>

<sup>1,2,3</sup>Optimized thermal Systems, Inc.

7040 Virginia Manor Road, Beltsville, MD, 20705

<sup>3</sup>Center for Environmental Energy Engineering

Department of Mechanical Engineering, University of Maryland  
College Park, MD, 20742

Email: <sup>1</sup>[sarpotdar@optimizedthermalsystems.com](mailto:sarpotdar@optimizedthermalsystems.com), <sup>2</sup>[nasuta@optimizedthermalsystems.com](mailto:nasuta@optimizedthermalsystems.com),  
<sup>3</sup>[vikrant@umd.edu](mailto:vikrant@umd.edu)

\* Corresponding Author

### ABSTRACT

In recent years, small diameter (less than 5 mm) microfin copper tubes have emerged as a better alternative to large diameter (7 mm and above) copper tubes. The superior performance of these small diameter tubes comes from their lower drag, and increased heat transfer coefficient. This results in heat exchangers with lightweight, compact designs, lower material cost, and reduced refrigerant charge compared to their large diameter counterparts. One of the prerequisites before one can design any heat exchanger is the characterization of fin and tube performance in terms of heat transfer and pressure drop correlations. The present literature lacks these correlations, especially the ones that can be used over a wide range of parameter space, for heat exchangers using louver fins and tube outer diameters of 5 mm and below. In this work we address that by undertaking a Computational Fluid Dynamics (CFD) study wherein we parametrize the louver fin design and evaluate the performance of these designs by running multiple CFD simulations in parallel. The study focuses on 3 mm to 5 mm diameter tubes with varying design parameters such as transverse and longitudinal tube pitch, number of tube banks, number of louvers, air velocity. We utilize Design of Experiments (DOE) methodologies including two level full factorial and latin hypercube sampling to efficiently sample the design space. Using the data generated from more than 1000 simulations, air side heat transfer and pressure drop correlations are developed. Multiple linear regression analysis is performed to develop Colburn  $j$  factor and Darcy  $f$  factor correlations. The new correlation reproduces 90% of the CFD data within 85% accuracy for heat transfer coefficient. For pressure drop the new correlation reproduces 90% of the CFD data within 90% accuracy. Work is underway to physically test the small diameter tube coils with louvered fins. The heat transfer and pressure drop data obtained through this physical testing will be used to further refine the aforementioned correlations.

### 1. INTRODUCTION

The refrigeration and air conditioning industry is experiencing constant pressure to make air-to-refrigerant heat exchangers more compact, cheaper and more energy efficient. There is also a need to develop heat exchangers that use reduced refrigerant charge, so as to reduce the impact of global warming of high Global Warming Potential (GWP) refrigerants, as well to reduce the safety risks associated with flammable refrigerants. Tube and fin heat exchangers are widely used in the HVAC&R industry. Reducing the diameter of the tube is one approach to achieve these objectives in tube and fin heat exchangers. Smaller tube diameters have smaller wake; this results in lower drag, making them more energy efficient. The smaller cross section of the smaller tubes can also be used to reduce the refrigerant charge. Hence, smaller tube diameter (< 5 mm) heat exchangers are proving to be superior alternatives to large diameter (>7mm) tube heat exchangers.

One of the prerequisites of designing and optimizing any heat exchanger is the availability of pressure drop and Heat Transfer Coefficient (HTC) correlations. Wang et al. (1999) developed correlations for louvered fins, for tube diameters ranging from 6.9 mm to 10.4 mm. Wu et al. (2012) performed CFD simulations as well as physical testing to develop a correlation for  $j$  factor that is applicable to louver fin heat exchangers with 5 mm tubes. However, the

parameter range for which they proposed this correlation was very restricted and they did not propose any correlation for  $f$  factor. Bacellar et al. (2014, 2015) developed correlations for bare tubes, flat fins and wavy fins for tube diameters ranging from 2 mm to 5mm. They followed a CFD simulation-based approach to develop these correlations. To best of our knowledge the present literature lacks a rigorous correlation that can characterize the performance of small tube diameter louvered fin heat exchangers, as such, that is the focus of this paper.

The outline of the present paper is as follows: we first give the details of the design space then give the outline of the data reduction technique used to obtain  $j$  and  $f$  factors from the raw CFD data. We then give the details of the CFD model that we used in this study. We also show sample CFD results illustrating the heat transfer enhancement mechanism of louvered fins. We then review the methodology that was used to develop  $j$  and  $f$  factor correlations. Finally we present statistical data associated with the accuracy of these correlations.

## 2. HEAT EXCHANGER MODELING AND DATA REDUCTION

There are several different parameters that can influence the performance of the louvered fin heat exchanger. In this study there are seven geometrical and one flow parameter that are under investigation. Table 1 lists these parameters, along with some pertinent additional information. Inputs from heat exchanger manufacturers are taken into account while setting the minima and maxima of these parameters (e.g., Louver pitch,  $L_p$ ) or setting up the relationship between different parameters (e.g.,  $C_l$  and  $C_t$ ). Based on the inputs from the manufacturers louver angle is kept constant, i.e.,  $27^\circ$ . Figure 1 shows the definitions of these parameters on a louver fin drawing. Note that as shown in Fig. 1, we restrict ourselves to the staggered tube arrangement.

**Table 1:** Heat exchangers design space.

Design Variable	unit	Min to Max
$D_n$	mm	3 to 5
$D_c$	mm	$(1.023+0.1)+2 \delta_f$
$C_l = P_l/D_n$	--	2 to 4
$C_t = P_t/P_l$	--	1 to 2
$N$	--	1 to 6
$N_l$	--	2 to 8
$FPI$	--	14 to 40
$L_p$	mm	0.8 to 1.8
$\theta$	degrees	27
$u$	m/s	0.75 to 5
$\delta_f$	mm	0.125

For data reduction we follow the methodology used by Bacellar et al. (2014), which is based on the work of Wang and Chi (2000) and Wang et al. (2000). The overall heat transfer coefficient ( $U$ ) is estimated using LMTD (eq.(1) to (3)).

$$\dot{Q} = \dot{m} \cdot c_{p,olr} \cdot (T_{air,out} - T_{air,in}) \quad (1)$$

$$\dot{Q} = UA_o \cdot LMTD \quad (2)$$

$$LMTD = \frac{(T_w - T_{air,in}) - (T_w - T_{air,out})}{\ln \left( \frac{T_w - T_{air,in}}{T_w - T_{air,out}} \right)} \quad (3)$$

As shown in equation (4) by Wang and Chi (2000), the thermal resistance associated with  $UA_o$  is a sum of all thermal resistances, as heat flows from the refrigerant at some bulk temperature to the air at some free stream temperature.

$$\frac{1}{UA_o} = \frac{1}{\eta_0 h_{air} A_o} + \frac{1}{2} \ln \left( \frac{D_o}{D_i} \right) \frac{D_o}{k_w A_w} + \frac{1}{h_{ref} A_{ref}} \quad (4)$$

As per Bacellar et al. (2014) one can neglect wall and refrigerant-side resistance when the tube wall temperature is fixed as a boundary condition in the CFD model. Thus equation (4) reduces to:

$$h_{air} = \frac{U}{\eta_o} \quad (5)$$

Here fin effectiveness ( $\eta_o$ ) is evaluated using iterative method outlined in Wang and Chi (2000).

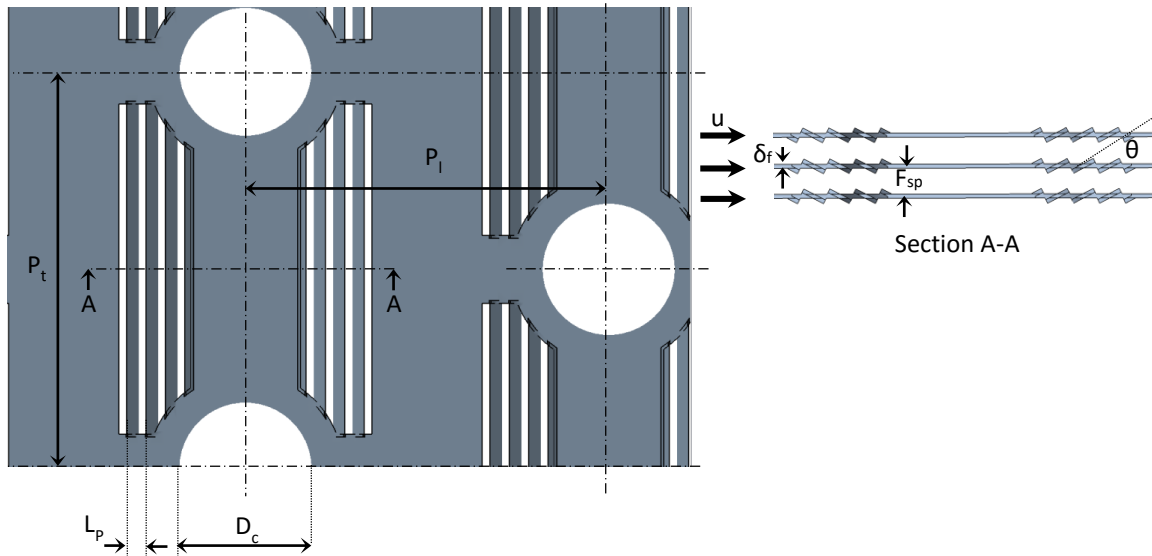


**Figure 1:** Louver fin parameters

The Colburn  $j$  factor is determined based on maximum velocity ( $u_{max} = u_{fr}/\sigma$ ) and is given by the following equation

$$j = \frac{h_{air} Pr^2}{\rho_m u_{max} c_{p_m}} \quad (6)$$

The friction factor is calculated based on the definition of Wang and Chi (2000), with the modification that is based on maximum velocity.

$$f = \frac{A_{min} \rho_m}{A_o \rho_l} \left[ \frac{2\Delta P \rho_l}{G_{max}^2} (1 + \sigma^2) \left[ \frac{\rho_l}{\rho_2} - 1 \right] \right] \quad (7)$$

Here the air side pressure drop is obtained from air mass-weighted average pressures at inlet and outlet ( $\Delta P = P_{in} - P_{out}$ ).

### 3. CFD MODELING

CFD simulations are performed using commercial CFD software STAR CCM<sup>+</sup>®. Figure 2a shows the CFD boundary conditions. As shown in the figure, flow enters the CFD domain through a velocity inlet boundary condition and leaves the domain through a pressure outlet boundary condition. The top and bottom of the domain are set as symmetry boundary conditions. The CFD domain is set up in such a way that fins, with half fin thickness, are on the sides. Thus the right half of the louver is on the right side of the domain and the left half of the louver is on the left side. It is through the periodic boundary condition that the flow from left side of the louver communicates with the right hand side of the louver and vice versa. Note that the air enters the CFD domain at 35° C and the tube walls are set at 65° C.

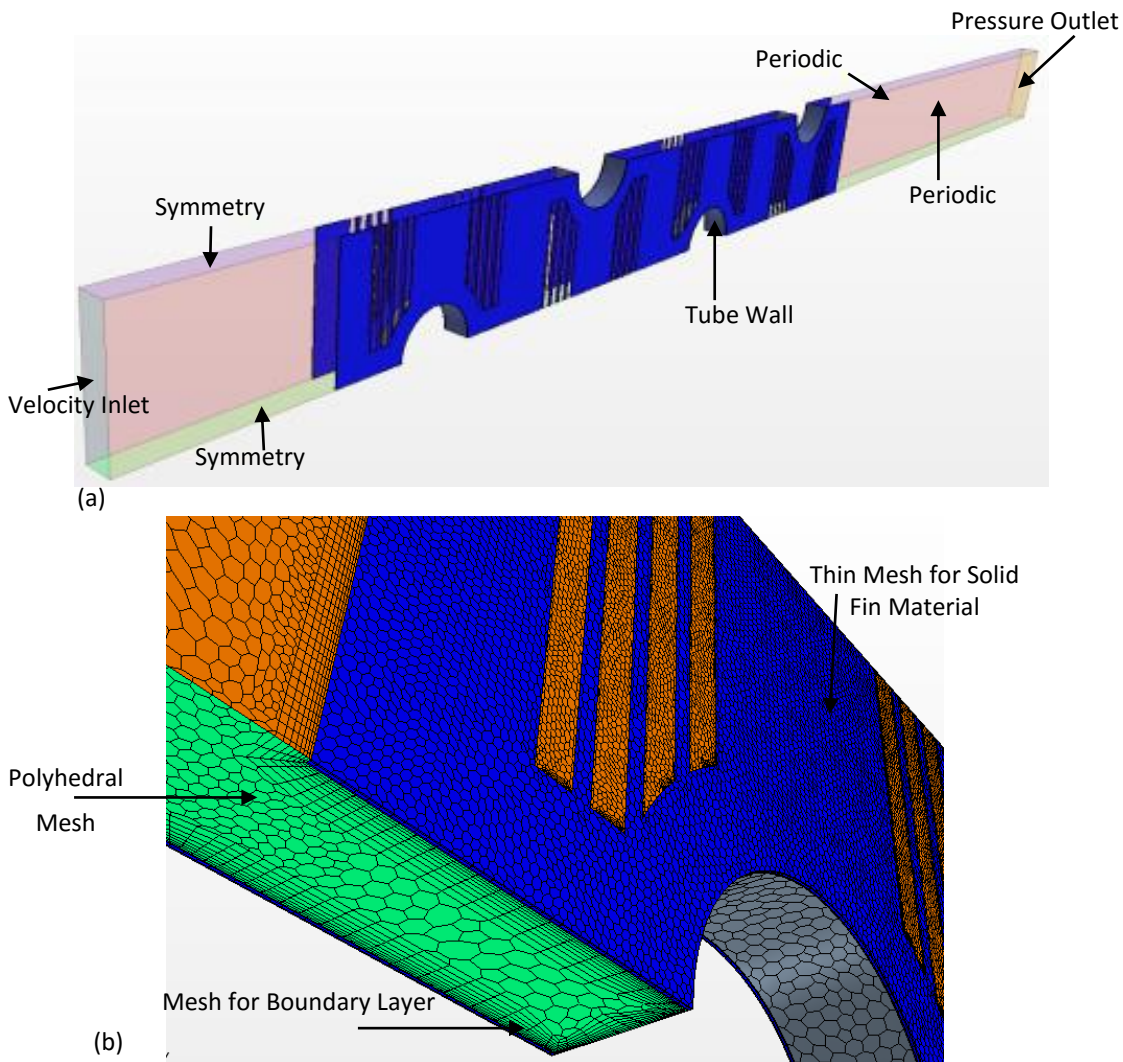


**Figure 2:** CFD (a) boundary conditions and (b) mesh

Figure 2b shows the mesh. As shown in the figure we use a polyhedral mesh for the core. To resolve the boundary layer, along the fin and tube walls, a boundary layer mesh is used. Note that the fin (shown as blue) is modeled as a separate continua through a *thin* mesh. The air is modeled as an ideal gas. Properties such as thermal conductivity, specific heat are assumed to be constant. Two layer SST  $K-\omega$  model was used for turbulence modeling. Segregated temperature fluid solver was used to solve the energy and momentum equations. Second order discretization scheme was employed to solve all the equations, viz., momentum, energy and turbulence.

It is the tube wall that is responsible for transferring heat to the air that enters the CFD domain. A part of this heat flux comes from the direct contact between the tube wall and air, whereas the rest is transferred via conduction through the fin material. Segregated solid energy solver with second order discretization was used to simulate the conduction through the fins. Aluminum is set as the fin material.

### 3.1 Mesh Independence Study

A mesh independence study is performed to ensure that the results are not influenced by the size of the mesh chosen. Grid Convergence Index (GCI) calculated based on Richardson Extrapolation method (Roach, 1997, ASME, 2009) is used to assess the mesh independence. Since the number of cases simulated in this study are very large

(1000+), only cases on the boundaries of the design space are scrutinized for mesh independence analysis. For each case, a set of three grids, with element size ratio ( $r_g = \Delta h_{\text{coarse}} / \Delta h_{\text{fine}}$ ) 1.35, are used for simulation. The observed order of accuracy ( $p$ ) is limited between 0.5 and 2.0 to avoid biased uncertainty determination (Oberkampf and Roy, 2010). Figure 3 shows results for GCI for both pressure drop and HTC. The mean uncertainty in the pressure drop and HTC was found to be 1.5 % and 1.1% respectively.

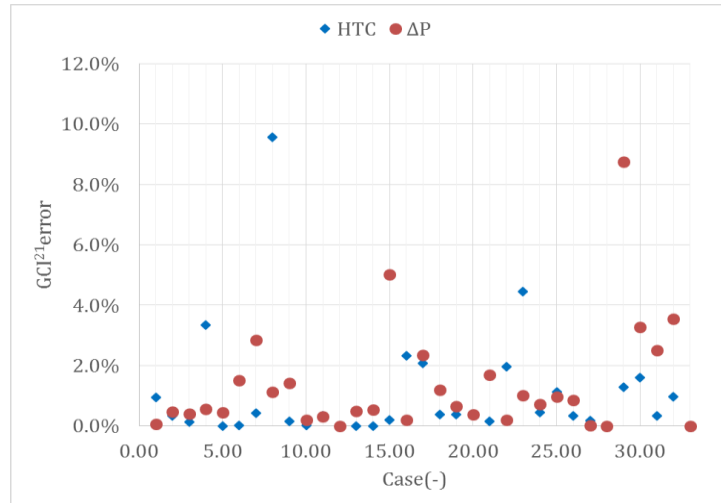


**Figure 3:** Mesh independence analysis (in  $GCI^{21}$  Superscript 2 denotes baseline mesh and 1 denotes finer mesh)

### 3.2 CFD Results

Figure 4 shows CFD results for one of the sample cases. Figure 4a shows a temperature contour plot on the surface of the fin. Note that interruption caused by the louvers inhibits the heat conduction which is responsible for relatively low temperature at both ends of the fins. Figure 4b shows convective heat flux on both sides of the fin. Note that compared to the right side, the left side of the fin surface, immediately downstream of the first louver, exhibits high heat flux. This is because on the left side, the louver is able to intercept the free stream and force it to restart a boundary layer with steep thermal gradient just downstream. A similar observation can be made downstream of the second louver but on the right side of the fin.

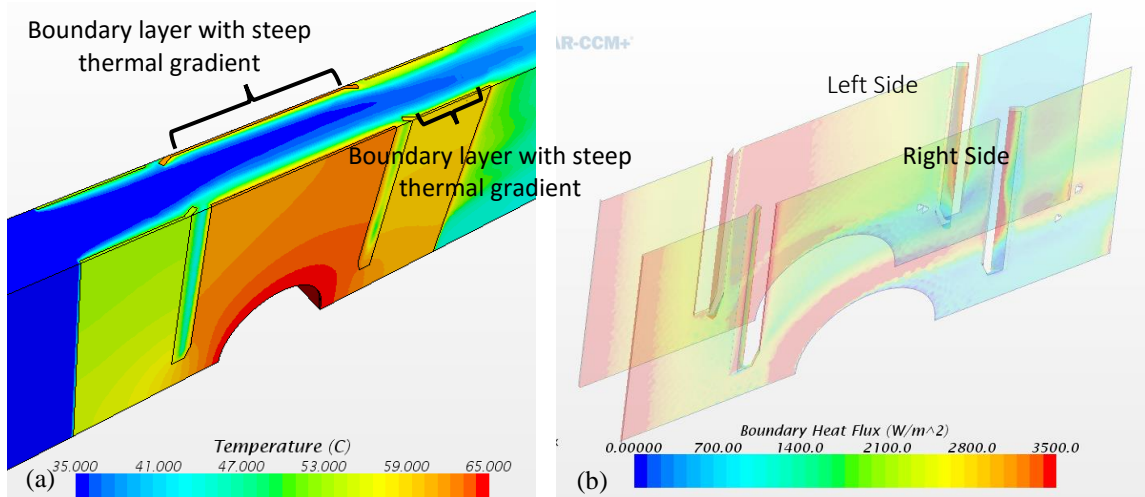


**Figure 4:** Sample CFD Results (flow is going from left to right)

Table 1 gives the design parameter space under consideration for the louver fin. This design space was sampled using two level full factorial method. In addition to that 1000 designs were sampled using latin hypercube sampling

technique, yielding a total of 1256 design points. Any designs involving infeasible design parameters were eliminated before they were simulated, e.g., designs wherein louvers were interfering with the tubes. After eliminating the infeasible design there were still more than 1000 sample points to be simulated. These simulations were run in parallel to reduce the total computation time. For the residuals of continuity, momentum and energy equations convergence criterion of  $1e-6$  was used. Static pressure at the inlet and static temperature at the outlet were also monitored to make sure they reach a steady state value. Figure 5 shows the results for  $f$  and  $j$  factors from these simulations.

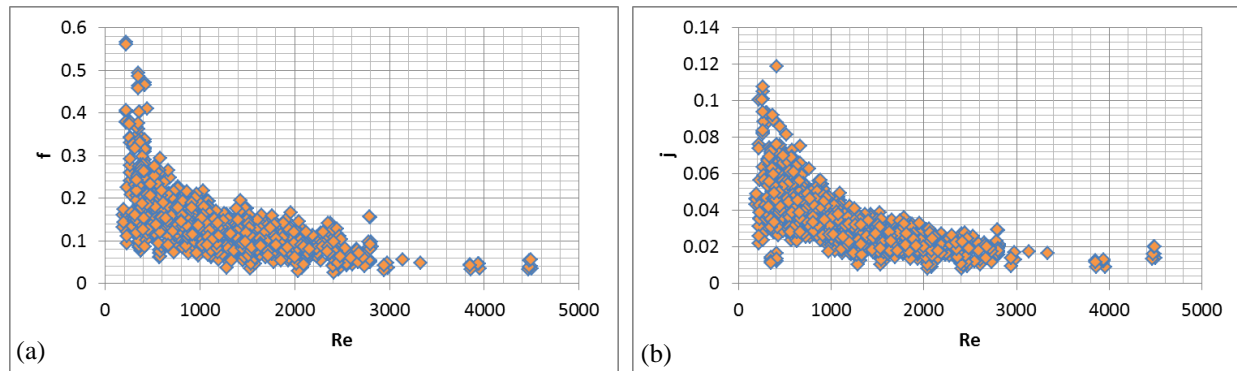


Figure 5: CFD Results

#### 4. CORRELATION DEVELOPMENT

An attempt was made to correlate the data with the equations published by Wang et al. (1999) for louver fin heat exchangers. However, this approach resulted in poor agreement between predicted and simulated results. A new form of correlation was found necessary to fit the data collected from this CFD study. This process can often be challenging and time-consuming. Because this team will also supplement these results with experimental work in the near future, a temporary correlation is proposed using a simple linear regression approach with a relatively large number of terms. MATLAB's stepwiselm algorithm was used to build these correlations. The algorithm adds and removes input variables one at a time until it cannot improve the fit any further. It also evaluates the effect of interaction of two terms, if it improves the accuracy of the model then that interaction term is retained, otherwise it is not included in the model. All data are log transformed to prevent negative predictions; a generic form of the correlation model is as follows.

$$\ln(Z) = \sum \ln(X_i) \ln(Y_i) m_i \quad (8)$$

Where  $Z$  is the model response e.g.,  $j$  or  $f$ ;  $X_i$  and  $Y_i$  are the  $i$ <sup>th</sup> input predictor terms; and  $m_i$  is their coefficient. Table 2 lists  $X_i$  and  $Y_i$  and corresponding  $m_i$ , for the friction factor correlation. The  $j$  correlation is obtained in two steps. As a first step a correlation for an intermediate term,  $\eta$ , is obtained. To avoid confusion with the actual fin efficiency  $\eta$ , the "efficiency estimator" is referred to as  $\eta_{estimator}$ . Refer to the Table 3 for the definition of  $\eta_{estimator}$ . The  $\eta_{estimator}$  is then used as one of the input parameters to build the  $j$  correlation. Table 4 gives the definition of the  $j$  correlation model. The  $f$  correlation can predict 93.1 % of the CFD data within 90% of accuracy. The  $j$  correlation can predict 84.7% of the data with 90% accuracy. Table 5 lists some of the other relevant statistics associated with the accuracy of these correlations. Figure 6 shows regression plots for pressure drop and HTC. The results shown in this figure are in line with the statistics presented in Table 5. The correlation validation mentioned here is performed with the same CFD data that was used to construct these correlations. In order to make sure these correlations behave as expected, an additional 117 designs were sampled randomly. Comparison between the CFD results and the correlation showed that the accuracy of these correlation in predicting the pressure drop and HTC of the random designs is very close to the statistics mentioned in Table 5. The  $f$  correlation can predict pressure drop for 93.7% of the randomly sampled designs with 90% or accuracy, whereas  $j$  correlation can predict the HTC for 83.8% of the designs with 90% accuracy.

Table 2:  $f$  correlation

X,Y	m	X,Y	m	X,Y	m
P <sub>i</sub> ,e	-1013669.2878	N , F <sub>p</sub>	-479333.6387	L <sub>h</sub> , D <sub>c</sub>	259.8500
P <sub>t</sub> ,e	-1345777.7429	N , L <sub>h</sub>	158.4946	L <sub>h</sub> , D <sub>h</sub>	-459.8980
N,e	-1345602.6806	N , D <sub>c</sub>	-8.4423	L <sub>h</sub> ,A <sub>o</sub>	-159.0586
L <sub>p</sub> ,e	-364221.9026	N , D <sub>h</sub>	479333.5205	L <sub>h</sub> , σ	272.4604
N <sub>i</sub> ,e	-173875.8253	N ,A <sub>o</sub>	479301.2725	L <sub>h</sub> ,φ	170.8954
F <sub>p</sub> ,e	-1344974.3361	N ,Re	-0.4219	D <sub>c</sub> , D <sub>h</sub>	36.6127
L <sub>h</sub> ,e	2617.1979	N , σ	-479306.7790	D <sub>c</sub> ,A <sub>o</sub>	8.6218
D <sub>c</sub> ,e	483.1974	L <sub>p</sub> , N <sub>i</sub>	3.0912	D <sub>c</sub> ,Re	-0.2043
D <sub>h</sub> ,e	1344955.2477	L <sub>p</sub> , F <sub>p</sub>	-521962.5255	D <sub>c</sub> ,φ	-9.9323
A <sub>o</sub> ,e	1345602.4009	L <sub>p</sub> , L <sub>h</sub>	194.5016	D <sub>h</sub> ,A <sub>o</sub>	-479333.9745
A <sub>min</sub> ,e	13.4232	L <sub>p</sub> , D <sub>c</sub>	-204.6995	D <sub>h</sub> ,Re	0.2273
Re,e	-2.2923	L <sub>p</sub> , D <sub>h</sub>	521960.2414	D <sub>h</sub> , σ	479309.3599
σ,e	-1345307.1332	L <sub>p</sub> ,A <sub>o</sub>	521716.8173	D <sub>h</sub> ,φ	39.3472
φ,e	309.1139	L <sub>p</sub> ,Re	0.0266	A <sub>o</sub> ,Re	0.4106
P <sub>i</sub> , L <sub>p</sub>	-521591.6158	L <sub>p</sub> , σ	-521811.4140	A <sub>o</sub> , σ	479307.1452
P <sub>i</sub> , N <sub>i</sub>	-250824.7612	L <sub>p</sub> ,φ	-134.2064	Re, σ	-0.1820
P <sub>i</sub> ,Re	-0.5617	N <sub>i</sub> , F <sub>p</sub>	-250817.2097	σ ,φ	-19.0630
P <sub>i</sub> ,φ	2.9407	N <sub>i</sub> , L <sub>h</sub>	-3.8068	P <sub>i</sub> , P <sub>i</sub>	239648.2676
P <sub>t</sub> , N	-479302.9909	N <sub>i</sub> , D <sub>c</sub>	-0.2371	P <sub>t</sub> , P <sub>t</sub>	-239655.0680
P <sub>t</sub> , L <sub>p</sub>	-521647.1302	N <sub>i</sub> , D <sub>h</sub>	250827.3445	N , N	-239650.6078
P <sub>t</sub> , N <sub>i</sub>	-250814.8012	N <sub>i</sub> ,A <sub>o</sub>	250824.8064	L <sub>p</sub> , L <sub>p</sub>	-229.1913
P <sub>t</sub> , F <sub>p</sub>	-479331.3620	N <sub>i</sub> , A <sub>min</sub>	-10.0744	N <sub>i</sub> , N <sub>i</sub>	0.1158
P <sub>t</sub> , L <sub>h</sub>	70.0900	N <sub>i</sub> ,Re	0.0876	F <sub>p</sub> , F <sub>p</sub>	-239687.8623
P <sub>t</sub> , D <sub>h</sub>	479330.2085	N <sub>i</sub> , σ	-250816.4603	D <sub>c</sub> , D <sub>c</sub>	-12.8649
P <sub>t</sub> ,A <sub>o</sub>	479302.9370	F <sub>p</sub> , L <sub>h</sub>	463.9202	D <sub>h</sub> , D <sub>h</sub>	-239687.0501
P <sub>t</sub> ,Re	-0.4255	F <sub>p</sub> , D <sub>c</sub>	-36.1484	A <sub>o</sub> ,A <sub>o</sub>	-239650.6353
P <sub>t</sub> , σ	-479313.7700	F <sub>p</sub> , D <sub>h</sub>	479373.5574	Re,Re	0.1058
N , L <sub>p</sub>	-521716.3659	F <sub>p</sub> ,A <sub>o</sub>	479334.0663	σ , σ	-239638.7552
N , N <sub>i</sub>	-250824.8020	F <sub>p</sub> , σ	-479306.0537	e,e	815760.3348

Table 3: Fin efficiency estimator correlation

X,Y	m	X,Y	m	X,Y	m
P <sub>i</sub> ,e	-18565659.01122	P <sub>t</sub> ,Re	78990.62947	F <sub>p</sub> ,A <sub>min</sub>	-191825.89638
P <sub>t</sub> ,e	-18565604.17865	P <sub>t</sub> ,σ	628523.38379	F <sub>p</sub> ,Re	78990.01396
N,e	-18565647.48194	N,L <sub>p</sub>	6401525.16690	F <sub>p</sub> ,σ	628529.55895
L <sub>p</sub> ,e	4437161.05822	N,N <sub>i</sub>	69546.25039	L <sub>h</sub> ,D <sub>h</sub>	7966249.80713
N <sub>i</sub> ,e	48210.21106	N,F <sub>p</sub>	2.27171	L <sub>h</sub> ,A <sub>o</sub>	7966267.20778
F <sub>p</sub> ,e	-18565563.23790	N,L <sub>h</sub>	-7966265.77006	L <sub>h</sub> ,Re	-1.16423
L <sub>h</sub> ,e	-5521760.42376	N,D <sub>c</sub>	0.02876	L <sub>h</sub> ,σ	-7966258.42544
D <sub>c</sub> ,e	15.67447	N,D <sub>h</sub>	-2.45527	L <sub>h</sub> ,φ	-0.09130
D <sub>h</sub> ,e	18565617.09720	N,A <sub>o</sub>	0.02272	D <sub>c</sub> ,Re	-0.45932
A <sub>o</sub> ,e	18565652.28343	N,A <sub>min</sub>	-191823.61809	D <sub>c</sub> ,φ	-2.32638
A <sub>min</sub> ,e	-133017.44334	N,Re	78990.49039	D <sub>h</sub> ,A <sub>o</sub>	2.11917
Re,e	54749.09228	N,σ	628532.39001	D <sub>h</sub> ,A <sub>min</sub>	191820.55396
σ,e	-18129911.70921	L <sub>p</sub> ,N <sub>i</sub>	-0.72558	D <sub>h</sub> ,Re	-78989.99048
φ,e	9.31797	L <sub>p</sub> ,F <sub>p</sub>	6401512.79528	D <sub>h</sub> ,σ	-628544.20373
P <sub>i</sub> ,L <sub>p</sub>	6401525.77629	L <sub>p</sub> ,L <sub>h</sub>	-0.85234	A <sub>o</sub> ,A <sub>min</sub>	191825.67180
P <sub>i</sub> ,N <sub>i</sub>	69546.25082	L <sub>p</sub> ,D <sub>h</sub>	-6401513.17382	A <sub>o</sub> ,Re	-78990.51967
P <sub>i</sub> ,L <sub>h</sub>	-7966266.51841	L <sub>p</sub> ,A <sub>o</sub>	-6401526.30491	A <sub>o</sub> ,σ	-628534.21211
P <sub>i</sub> ,D <sub>c</sub>	3.41450	L <sub>p</sub> ,Re	0.92156	A <sub>min</sub> ,σ	-191805.50245
P <sub>i</sub> ,A <sub>min</sub>	-191823.84565	L <sub>p</sub> ,σ	6401519.98263	A <sub>min</sub> ,φ	-0.25348
P <sub>i</sub> ,Re	78990.76907	N <sub>i</sub> ,F <sub>p</sub>	69543.60000	Re,σ	78990.34381

$P_i, \sigma$	628530.84024	$N_i, L_h$	0.89805	$Re, \varphi$	-0.34930
$P_i, \varphi$	3.47680	$N_i, D_h$	-69546.68518	$\sigma, \varphi$	2.14235
$P_t, L_p$	6401523.91133	$N_i, A_o$	-69546.24518	$P_t, P_t$	-1.90161
$P_t, N_i$	69543.20522	$N_t, A_{min}$	3.07463	$P_t, P_t$	10.67160
$P_t, F_p$	14.67942	$N_i, Re$	-0.01708	$N_i, N_i$	-0.02281
$P_t, L_h$	-7966264.16576	$N_i, \sigma$	69543.47506	$F_p, F_p$	12.52578
$P_t, D_c$	-2.43865	$N_i, \varphi$	-0.03965	$D_h, D_h$	12.21223
$P_t, A_o$	-2.06495	$F_p, L_h$	-7966249.47557	$\sigma, \sigma$	628518.22988
$P_t, A_{min}$	-191833.16220	$F_p, D_h$	-19.09811	$\varphi, \varphi$	-1.67822
$e, e$	-12868725.24338				

Table 4:  $j$  correlation

$X, Y$	$m$	$X, Y$	$m$	$X, Y$	$m$
$P_t, e$	-4643227.1858	$P_t, A_o$	48.9549	$L_h, D_c$	4.9860
$P_t, e$	-4643603.4143	$P_t, A_{min}$	93.5378	$L_h, D_h$	629364.5911
$N, e$	-4643111.1017	$P_t, Re$	3.1323	$L_h, A_o$	629516.4040
$L_p, e$	-86.4348	$P_t, \sigma$	-529.0520	$L_h, \sigma$	-629415.0751
$N_i, e$	-0.9530	$P_t, \varphi$	-21.5283	$L_h, \varphi$	3.6528
$F_p, e$	-4642797.6584	$P_t, \eta_{estimator}$	-8.0638	$D_c, D_h$	11.4127
$L_h, e$	-436235.6492	$N, L_h$	-629516.4403	$D_c, A_o$	48.7957
$D_c, e$	91.5408	$N, D_c$	-48.2122	$D_c, Re$	-7.0628
$D_h, e$	4641953.2439	$N, D_h$	-573.9676	$D_c, \varphi$	18.8867
$A_o, e$	4643125.6075	$N, A_o$	-10.0176	$D_c, \eta_{estimator}$	-74.8642
$A_{min}, e$	474.4170	$N, A_{min}$	45.3350	$D_h, A_o$	564.1703
$Re, e$	-3.0271	$N, Re$	-0.1279	$D_h, A_{min}$	-662.4413
$\sigma, e$	-4643074.1006	$N, \eta_{estimator}$	-41.4151	$D_h, \eta_{estimator}$	26.5354
$\varphi, e$	63.7023	$L_p, F_p$	-115.4164	$A_o, A_{min}$	-35.4613
$\eta_{estimator}, e$	-50.7932	$L_p, D_h$	119.7620	$A_o, \eta_{estimator}$	40.0599
$P_t, N_i$	1.7939	$L_p, Re$	0.1414	$A_{min}, \sigma$	438.6684
$P_t, L_h$	-629519.4423	$L_p, \sigma$	-81.4239	$Re, \sigma$	1.9837
$P_t, D_c$	-80.7474	$L_p, \eta_{estimator}$	0.9211	$Re, \varphi$	-4.4837
$P_t, D_h$	-534.6311	$N_i, L_h$	0.0690	$Re, \eta_{estimator}$	1.6061
$P_t, A_o$	9.7853	$N_i, D_c$	-3.3218	$\sigma, \varphi$	16.2567
$P_t, Re$	3.6938	$N_i, A_o$	-0.0626	$\varphi, \eta_{estimator}$	-50.4474
$P_t, \varphi$	-12.0748	$N_i, Re$	0.1054	$P_t, P_t$	-92.4998
$P_t, N$	-49.2971	$N_i, \sigma$	1.0381	$N, N$	10.0627
$P_t, L_p$	-11.1450	$N_i, \varphi$	-2.1297	$F_p, F_p$	-601.3794
$P_t, N_i$	1.5264	$N_i, \eta_{estimator}$	0.6601	$D_c, D_c$	27.1121
$P_t, F_p$	-759.2152	$F_p, L_h$	-629369.6219	$D_h, D_h$	599.0926
$P_t, L_h$	-629504.2112	$F_p, A_{min}$	665.1553	$Re, Re$	0.0886
$P_t, D_c$	-91.9804	$F_p, \sigma$	-976.7907	$\sigma, \sigma$	-379.3282
$P_t, D_h$	128.3568	$F_p, \varphi$	7.4727	$e, e$	-3217786.2245

Table 5: Overall Results: Percent of designs with less than the specified deviation

	$\Delta P$	HTC
10% absolute deviation	93.1%	84.7%
15% absolute deviation	98.7%	93.9%
20% absolute deviation	99.8%	97.4%
Mean GCI <sup>21*</sup>	1.5%	1.1%

\* Superscript 2 denotes baseline mesh and 1 denotes finer mesh

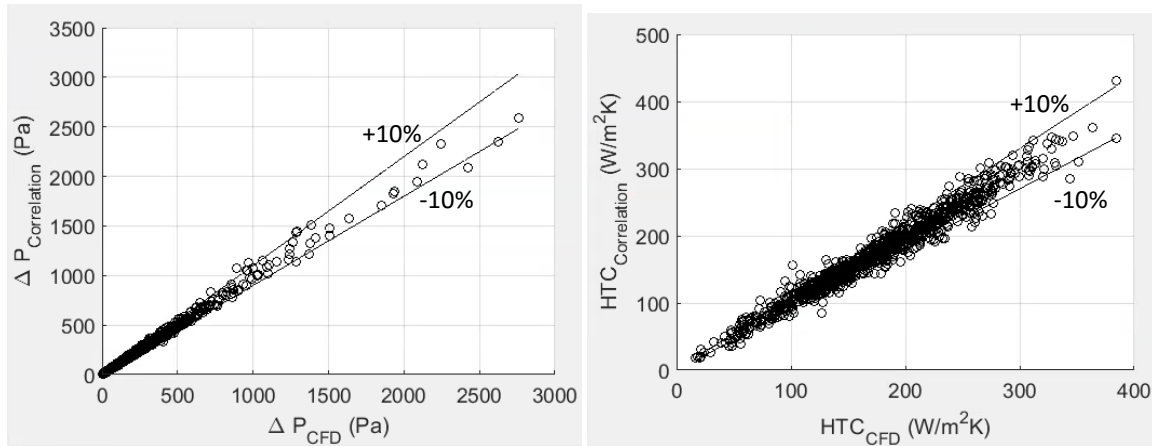


**Figure 6:** Verification of the correlations against the CFD data. (a) pressure drop; (b) heat transfer coefficient

## 5. CONCLUSIONS

The paper presents pressure drop and heat transfer coefficient correlations for small diameter (3mm to 5mm) tube louvered fins. More than 1000 designs are sampled using augmented two level full factorial sampling technique.  $j$  and  $f$  factor for these designs are obtained via CFD simulations. Linear regression analysis is used to develop the correlations for  $j$  and  $f$  factor. The  $f$  correlation predicts 98.7% of the CFD data within 85% accuracy. The  $j$  correlation predicts 93.9% of the CFD data within 85% accuracy. Calibration of these correlations using data from the physical testing is underway. However, we believe that these correlations, in the form they are presented in this paper, are still very useful in designing and optimizing small diameter louvered fin heat exchangers.

### NOMENCLATURE

A	area	(m <sup>2</sup> )	k	thermal conductivity	(W/m.K)
A <sub>o</sub>	total (tube +fin) surface area	(m <sup>2</sup> )	L <sub>p</sub>	Louver pitch	(m or mm)*
c <sub>p</sub>	specific heat	(J/kg.K)	$\dot{m}$	mass flow rate	(kg/s)
D <sub>c</sub>	collar diameter	(m or mm)*	N	number of banks	(-)
D <sub>i</sub>	inner tube diameter	(m or mm)*	N <sub>l</sub>	number of louvers	(-)
D <sub>o</sub>	outer tube diameter	(m or mm)*	P	pressure	(Pa)
D <sub>n</sub>	nominal tube diameter	(m or mm)*	Pr	Prandtl number	(-)
e	Euler number (2.71828)	(-)	P <sub>t</sub>	transversal tube pitch	(m or mm)*
FPI	fins per inch	(-)	Q	heat rate	(W)
f	friction factor	(-)	Re	Reynold's no. ( $\rho u_{max} D_c / \mu$ )	(-)
G	mass flux	(kg/m <sup>2</sup> .s)	rg	mesh element size ratio	(-)
h	heat transfer coefficient	(W/m <sup>2</sup> .K)	T	temperature	(K)
h	mesh element size	(m or mm)*	u	velocity	(m/s)
j	colburn factor	(-)	UA <sub>o</sub>	overall HTC	(W/K)

### Greek letters

$\delta_f$	fin thickness	(m or mm)*
$\mu$	dynamic viscosity	(Pa·s)
$\eta$	fin efficiency	(-)
$\eta_o$	fin effectiveness	(-)
$\theta$	louver angle	(degrees)

### Subscripts

f	fin
fr	frontal
m	mean
max	maximum
ref	refrigerant

\*Unless otherwise mentioned the unit is meter

$\rho$	density (kg/m <sup>3</sup> )		$w$	wall
$\sigma$	contraction ratio	(-)		
$\varphi$	fin efficiency geometrical parameter	(-)		

## REFERENCES

- ASME. (2009). Standard for Verification and Validation in Computational Fluid Dynamics and Heat Transfer – Section 2: Code verification, *ASME V&V 20 Standard*, 7-17.
- Bacellar, D., Aute, V., Radermacher, R. (2014). CFD-Based correlation development for air side performance of finned and finless tube heat exchangers with small diameter tubes. *15<sup>th</sup> International Refrigeration and Air Conditioning Conference at Purdue University*, West Lafayette, Indiana, Paper 1410.
- Bacellar, D., Aute, V., Radermacher, R. (2015). CFD-based correlation development for air side performance on finned tube heat exchangers with wavy fins and small tube diameters, *24<sup>th</sup> IIR International Congress of Refrigeration*, Yokohama, Japan
- Oberkampf, W., and Roy, C. (2010). *Verification and Validation in Scientific Computing*, New York: Cambridge University Press.
- Roache, P. J. (1997). Quantification of uncertainty in computational fluid dynamics. *Annual Review of Fluid Mechanics*, 29, 123-160.
- Wu, W., Ding, G, Zheng, Y, Gao, Y, and Song, J. (2012). Principle of designing fin-and-tube heat exchanger with smaller tube for air condition. *International Refrigeration and Air Conditioning Conference at Purdue University*, West Lafayette, Indiana, Paper 1217.
- Wang, C, Lee, C., Chang, C., Lin, S. (1999). Heat transfer and friction correlation for compact louvered fin-and-tube heat exchangers, *International Journal of Heat and Mass Transfer*, 42, 1945-1956.
- Wang, C., Chi, K. (2000). Heat transfer and friction characteristics of plain fin-and-tube heat exchangers, part I: new experimental data, *International Journal of Heat and Mass Transfer*, 43, 2681-2691.
- Wang, C., Chi, K., Chang, C. (2000). Heat transfer and friction characteristics of plain fin-and-tube heat exchangers, part II: Correlation, *International Journal of Heat and Mass Transfer*, 43, 2693-2700.

## ACKNOWLEDGEMENT

The present work was supported by the International Copper Association. The authors acknowledge Hal Stillman from the International Copper Association, Yoram Shabtay from Heat Transfer Technologies, LLC and Roger Tetzloff from Burr Oak Tool for their valuable comments.